ELSEVIER

Computers and Chemical Engineering 24 (2000) 2457–2472

Computers & Chemical Engineering

www.elsevier.com/locate/compchemeng

Simulation of kinetic effects in reactive distillation

Fengrong Chen, Robert S. Huss, Michael F. Malone, Michael F. Doherty *

Department of Chemical Engineering, University of Massachusetts, Amherst, MA 01003, USA

Received 27 December 1999; received in revised form 29 June 2000; accepted 30 June 2000

Abstract

This paper describes a simulation and modeling methodology for kinetically controlled, stage-wise reactive distillation columns, taking into account equimolar or non-equimolar reactions, side-reactions, effects of heat of reaction, non-constant latent heat effects, a distribution of liquid holdups on the reactive stages and hybrid sections in a column. A Damköhler number, which is the ratio of a characteristic liquid residence time to a characteristic reaction time, is introduced into the mathematical model. By changing the Damköhler number, the transition behavior from the nonreactive to the equilibrium reactive limits can be described. Combining the model type and the holdup distribution type on the reactive stages, four simulation strategies are studied: (1) non-heat effects model and constant molar holdup; (2) non-heat effects model and non-constant molar holdup; (3) heat effects model and constant molar holdup; (4) heat effects model and non-constant molar holdup. These strategies can be used to handle very diverse reactive distillation systems. The modeling tool capabilities are demonstrated with case studies for the metathesis of 2-pentene, MTBE synthesis and the hydration of ethylene oxide to ethylene glycol. For MTBE synthesis, the output multiplicities present at chemical reaction equilibrium disappear at lower extents of reaction (i.e. at lower residence times or Damköhler numbers). © 2000 Elsevier Science Ltd. All rights reserved.

Keywords: Reactive distillation; Simulation; Metathesis of 2-pentene; MTBE; Ethylene glycol

1. Introduction

Reactive distillation is potentially an attractive process alternative to conventional liquid-phase chemical reaction processing for systems that exhibit one or more of the characteristics: equilibrium limited chemical reactions, exothermic reactions, poor raw materials usage due to selectivity losses, or excessive flowsheet complexity. Commercial reactive distillation processes such as the Nylon 6,6 process, methyl acetate process and MTBE process (Doherty & Buzad, 1992) have demonstrated reductions in capital investment and/or energy consumption.

Because of the potential benefits of this technology, the number of publications dealing with the theoretical and experimental performance of special reactive distillation process is rapidly increasing. Several parallel approaches are being developed to explore the effects of finite reaction rates. Despite the recent advances in design strategies achieved by many researchers (Barbosa & Doherty, 1988a,b; Rev, 1994; Buzad & Doherty, 1994, 1995; Sundmacher, Rihko & Hoffmann, 1994; Ciric & Gu, 1994; Ung & Doherty, 1995a; Espinosa, Aguirre & Perez, 1995a,b; Papalexandri & Pistikopoulos, 1996; Bessling, Schembecker & Simmrock, 1997; Nisoli, Malone & Doherty, 1997; Okasinski & Doherty, 1998; Hauan & Lien, 1998; Giessler, Danilov, Pisarenko, Serafimov, Hasebe & Hashimoto, 1998; Espinosa, Aguirre, Frey & Stichlmair, 1999; Bessling, 1999; Mahajani, 1999; Hauan, Westerberg & Lien, 2000; Lee, Hauan, Lien & Westerberg, 2000a,b; Melles, Grievink & Schrans, 2000), it is still difficult to bring a new reactive distillation process to production because of complexities in design, synthesis and operability of reactive distillation processes resulting from the interaction of reaction and distillation. Process analysis and operability are effectively treated through simulation, which is the main focus of this article.

There are many programs reported for steady-state and dynamic simulations of reactive distillation. Several methods have been presented for computing a single steady state or a transient-state, including tridiagonal

* Corresponding author. Tel.: +1-413-5450132; fax: +1-413-5451647.

E-mail address: mdoherty@ecs.umass.edu (M.F. Doherty).

0098-1354/00/$ - see front matter © 2000 Elsevier Science Ltd. All rights reserved.
PII: S0098-1354(00)00609-8

matrix methods (Suzuki, Yagi, Komatsu & Hirata, 1971; Izarraraz, Bentzen, Anthony & Holland, 1980; Tierney & Riquelme, 1982; Xu & Chen, 1987), Newton–Raphson methods (Nelson, 1971; Komatsu & Holland, 1977; Carra, Morbidelli, Santacesaria & Buzzi, 1979; Zhang, 1989), relaxation methods (Jelineck & Hlavacek, 1976; Komatsu, 1977; Grosser, Doherty & Malone, 1987; Bogacki, Alejski & Szymanowski, 1989), minimization method (Alejski, Szymanowski & Bogacki, 1988), inside-out algorithms (Venkataraman, Chan & Boston, 1990), homotopy-continuation method (Chang & Seader, 1988; Ciric & Miao, 1994), rate-based approach (i.e. including detailed hydraulics) (Sivasubramanian & Boston, 1990; Ruiz, Basualdo & Scenna, 1995; Higler, Taylor & Krishna, 1999) and equation oriented process approach with switching between steady-state and dynamic simulation modes (Gani, Perregaard & Johansen, 1990; Gani, Sørensen & Perregaard, 1992; Perregaard, Pedersen & Gani, 1992; Abufares & Douglas, 1995; Pilavachi, Schenk, Perrez-Cisneros & Gani, 1997; Sørensen, Johansen, Gani & Fredenslund, 1990).

Reactive distillation systems are bounded by two limiting cases: (1) the nonreactive case where no reaction occurs; and (2) the equilibrium reactive case where there is simultaneous vapor–liquid and reaction equilibrium. Kinetically controlled reactive distillation lies between these two limits and performance calculations that can track the transition between the two limits cases are desirable in design and analysis of such systems. However, the existing literature does not address such a simulation strategy for studying the transition behavior from the nonreactive to the equilibrium reactive limits. In a recent design approach (Doherty & Buzad, 1992; Venimadhavan, Buzad, Doherty & Malone, 1994; Buzad & Doherty, 1994, 1995; Okasinski & Doherty, 1998), a Damköhler number is used to characterize kinetically-limited systems. The Damköhler number is a dimensionless parameter defined as the ratio of a characteristic liquid residence time to a characteristic reaction time. Changing the Damköhler number means that the different separation scenarios between the two limiting cases can appear. In this paper the Damköhler number is introduced into our simulation model to study the transitions in performance of reactive distillation columns.

The aim of this work is to develop a systematic simulation methodology for kinetically controlled, stage-wise reactive distillation columns. This method can be used to perform rating calculations for chemical equilibrium designs, and has enough flexibility to investigate the possibilities of a column operating in the kinetic regime at any value of the Damköhler number. It takes into account equimolar or non-equimolar reactions, side-reactions, effects of heat of reaction, non-constant latent heat effects, a distribution of liquid holdups on the reactive stages and hybrid sections in a column. The model does not include effects due to column internals (e.g. pressure drops, flooding/weeping, etc). This enables us to simulate columns over a wide range of Damköhler numbers, and therefore, over the corresponding range of column diameters, weir heights, etc required to achieve the liquid holdups on each stage. Our simulations are intended to support the conceptual design of a reactive distillation column by providing more refined estimates of the number of stages in each column section (including hybrid sections), reflux and reboil ratios, flow rates, stage holdups, etc. This information may be used as input to the detailed equipment design (e.g. column diameter, tray type, etc).

First, the model equations are presented. Next, the solution strategy is described. Finally, the simulation results for several numerical examples (metathesis of 2-pentene, MTBE synthesis and ethylene glycol reactive system) are illustrated.

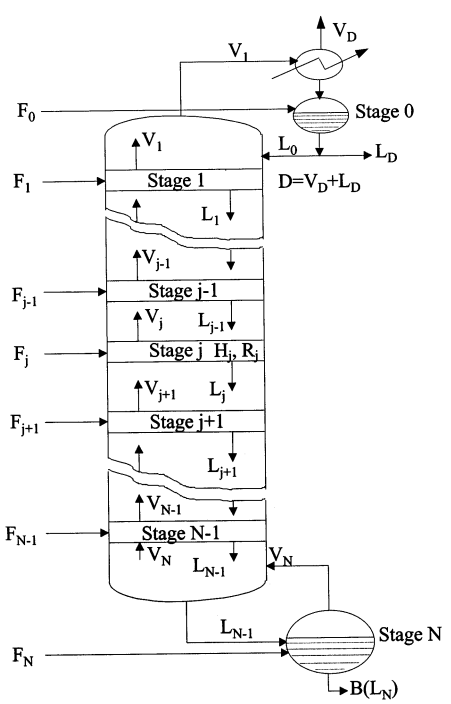

Fig. 1. Schematic representation of a reactive distillation column.

2. Model equations

Some reactive distillation systems have no obvious heat effects and others have significant heat effects. In this section, we develop two kinds of models: the *non-heat effects model* and the *heat effects model*. The following assumptions were made when formulating the model of the reactive distillation process illustrated in Fig. 1.

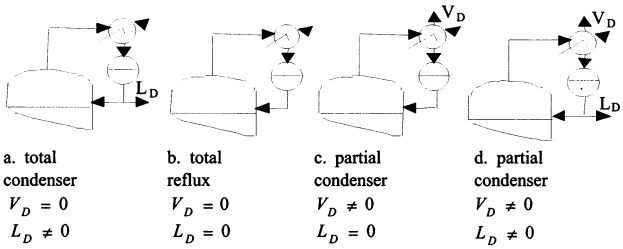

Fig. 2. Four types of condensers.

1. Four types of condensers (Fig. 2) are used.
2. Adiabatic column.
3. The molar heat of vaporization of the mixture is constant (**only for non-heat effects model**).
4. The heat of reaction is negligible compared to the heat of vaporization (**only for non-heat effects model**).
5. The reaction proceeds only in the liquid phase and is controlled by its kinetics.
6. Each stage is a perfectly mixed stirred-tank reactor (CSTR).
7. Vapor holdup is assumed to be negligible.
8. The vapor and liquid leaving any stage are in phase equilibrium.

Assumptions (1)–(8) are for the *non-heat effects model*. Assumptions (1)–(2) and (5)–(8) are for the *heat-effects model*. Both models have the same mass balance equations.

The mass balance for component i on a typical interior stage j $(j=1,\ldots,N-1;\ i=1,2,\ldots,c)$ is written in the unsteady-state form, and rearranging gives

$$\frac{\mathrm{d}x_{j,i}}{\mathrm{d}\tau}=\frac{H_T}{F}\frac{1}{H_j}(F_jz_{j,i}+L_{j-1}x_{j-1,i}+V_{j+1}y_{j+1,i}-V_jy_{j,i}-L_jx_{j,i})+\frac{H_T}{H_T^R}\frac{\mathrm{Da}}{k_{f,\mathrm{ref}}}\delta_j\sum_{r=1}^{R}(v_{r,i}\varepsilon_{j,r}) \tag{1}$$

where $\mathrm{d}\tau=(F/H_T)\,\mathrm{d}t$, $H_T=\Sigma_{j=0}^{N}H_j$, $H_T^R=\Sigma_{j=0}^{N}(\delta_jH_j)$. Here we introduce a parameter δ_j(0 or 1) to calculate the total reactive liquid holdup within a reactive column, H_T^R. When reaction occurs on stage j, δ_j is set to unity, otherwise $\delta_j=0$.

The Damköhler number, $\mathrm{Da}=(H_T^R/F)/(1/k_{f,\mathrm{ref}})=(H_T^Rk_{f,\mathrm{ref}})/F$, is a dimensionless ratio of a characteristic liquid residence time (H_T^R/F) to the characteristic reaction time $(1/k_{f,\mathrm{ref}})$. The quantity $k_{f,\mathrm{ref}}$ is the forward rate constant evaluated at a reference temperature, e.g. the boiling point of the lowest boiling pure component in the system. When $\mathrm{Da}\ll 1$ non-reactive distillation is recovered, and when $\mathrm{Da}\gg 1$, the equilibrium limit is approached.

It is convenient to reformulate Eq. (1) in terms of the parameter D, where $D=\dfrac{\mathrm{Da}}{1+\mathrm{Da}}$, which is well-scaled between 0 and 1, and the rescaled warped time $\mathrm{d}\zeta$, where $\mathrm{d}\zeta=(1+\mathrm{Da})\,\mathrm{d}\tau$.

$$\frac{\mathrm{d}x_{j,i}}{\mathrm{d}\zeta}=(1-D)\frac{H_T}{H_j}\frac{1}{F}(F_jz_{j,i}+L_{j-1}x_{j-1,i}+V_{j+1}y_{j+1,i}-V_jy_{j,i}-L_jx_{j,i})+D\frac{H_T}{H_T^R}\frac{1}{k_{f,\mathrm{ref}}}\delta_j\sum_{r=1}^{R}(v_{r,i}\varepsilon_{j,r}) \tag{2}$$

When $D=0$ Eq. (2) simplifies to the form for non-reactive distillation. As $D=1$, Eq. (2) simplifies to the form for phase and reaction equilibrium distillation.

The chemical reaction terms have been formulated based on a continuous perfectly mixed stirred-tank reactor and an activity-based rate expression. The total rate of generation of moles at stage j is given by

$$R_j=\delta_jH_j\sum_{r=1}^{R}(v_{T,r}\varepsilon_{j,r}),\quad j=0,1,\ldots,N \tag{3}$$

Where R is the number of reactions, and

$$\varepsilon_{j,r}=k_{f,r}\left(\prod_{i=1}^{C}a_{j,i}^{(|v_{r,i}|-v_{r,i})/2}-\frac{1}{K_r}\prod_{i=1}^{C}a_{j,i}^{(|v_{r,i}|+v_{r,i})/2}\right)$$
$$j=0,1,\ldots,N;\quad i=1,2,\ldots,C;\quad r=1,2,\ldots,R \tag{4}$$

$$v_{T,r}=v_{r,1}+v_{r,2}+\cdots+v_{r,C},\quad r=1,2,\ldots,R \tag{5}$$

Where the reaction equilibrium and reaction rate constants are expressed as

$$K_r=A_r\exp\left(\frac{B_r}{T}+C_r\ln(T)\right),\quad r=1,2,\ldots,R \tag{6}$$

$$k_{f,r}=a_r\exp\left(\frac{b_r}{T}\right),\quad r=1,2,\ldots,R \tag{7}$$

As shown in Eq. (1) or Eq. (2), the fundamental variables associated with each stage are the liquid and vapor flow rates, the liquid holdups, the extents of reaction, the stage compositions and temperature. The liquid and vapor flow rates throughout the column are calculated by the methods given in Appendix A.

3. Solution strategy

In this paper, four strategies are implemented in order to assess the effects of different model assumptions: (1) non-heat effects model and constant molar holdup distribution; (2) non-heat effects model and non-constant molar holdup distributions; (3) heat effects model and constant molar holdup distributions; (4) heat effects model and non-constant molar holdup

Table 1
Specification variables for different models and condenser configurations

Types	Specifications	
	Non-heat effects model	heat effects model
a. Total condenser	1. Reflux ratio, reboil ratio	1. Reflux ratio, L_D
	2. Reflux ratio, L_D	2. Reboil ratio, B
b. Total reflux	Reboil ratio, $r = \infty$	Reboil ratio, $r = \infty$
c. Partial condenser	1. Reflux ratio, reboil ratio	1. Reflux ratio, V_D
	2. Reflux ratio, V_D	2. Reboil ratio, B
d. Partial condenser	1. Reflux ratio, reboil ratio, V_D/F	1. Reflux ratio, D, V_D/F
	2. Reflux ratio, D, V_D/L_D	2. Reboil ratio, B, V_D/L_D

distributions. The column specifications for the simulation will change with the types of models (*non-heat effects model* or *heat effects model*), condensers and holdup distributions (constant molar holdup or non-constant molar holdup).

The common specification variables for a reactive column are the column pressure, the number of stages, the number of feeds, the feed composition, the feed quality, the feed rate, the feed locations, regardless of types of models, condensers and holdup distributions.

For the different type of condenser and mathematical model, some specification variables will change, except for the common specification variables listed above. Table 1 shows the changes of the specification variables for different models and condenser configurations.

For specifying the constant molar holdup distributions throughout a column, the value of the Damköhler number is used to calculate a total molar holdup for the column, which is then divided equally among all the reactive stages, including the condenser and reboiler. We allow two kinds of input for specifying the non-constant molar holdup distributions throughout a column: (1) The Damköhler number is specified and then used to calculate a total reactive molar holdup for the whole column from the definition ($\mathrm{Da} = H_T^R k_{f,\mathrm{ref}}/F$), then we specify the fraction of the total reactive molar holdup for each column stage with reactions. (2) We specify a volume holdup for each reactive stage, and the overall Damköhler number for the column is calculated after the simulation converges to steady-state.

For the simulation of a hybrid reactive column (i.e. some stages are reactive, others are non-reactive), the specification of reaction status for each column stage is necessary. We specify $\delta_j = 1$ or 0 to turn reaction on or off for each stage. The methods for specifying molar or volume holdups and reactive status for each column stage are shown in Table 2.

Though the specification variables are different for the different simulation strategies, the basic model equations are the same. In the above section, the mathematical models are represented by a mixed set of equations containing ordinary differential equations (ODEs) and algebraic equations. In order to solve numerically the set of ODEs and algebraic equations, the Backward Differentiation Formula (Gear, 1971) linear multistep methods for stiff systems are used. This approach is convenient for several reasons: (a) it is robust for arbitrary initializations, e.g. it has never failed to find a steady-state for any of the simulations we have attempted. (b) These models often have multiple steady states, and the dynamic simulator converges only to stable states, not to unstable states. (c) Most importantly, the model is very stiff in the limits of large Da, and the method is chosen to maximize accuracy and stability in this limit. The algorithm for solving the set of ODEs and algebraic equations is:

1. Specify all the common specifications for a reactive column and some special variables which relate to the types of models (*non-heat effects model* or *heat effects model*), condensers and holdup distributions as described above.

Table 2
Methods for specifying molar or volume holdups and reactive status for each column stage

Variables	Specification	
	Molar holdup (kg mol)	Volume holdup (m^3)
Damköhler number	Specify a value for $\mathrm{Da} = H_T^R k_{f,\mathrm{ref}}/F$	Calculated from converged simulation
Molar holdups on each stage	Specify the fraction of the total molar reactive holdup per stage	Calculate the molar holdup per stage from converged simulation
Volume holdups on each stage	Calculate the volume holdup per stage from converged simulation	Specify the volume holdup per stage
Reactive status on each stage	Specify 1 or 0*	Specify 1 or 0*

* 1 — stage has reactions; 0 — stage without reactions.

Table 3
Specifications for the simulation of the metathesis system

Number of stages		14
Feed location		6
Feed quality		1
Feed rate		100 kmol h^{-1}
Feed composition (mole fraction)	C_4H_8	0.0
	C_5H_{10}	1.0
	C_6H_{12}	0.0
Reflux ratio		4.0
Reboil ratio		5.0
Heat of reaction		0.0 kJ $kmol^{-1}$
Condenser type		a. Total condenser

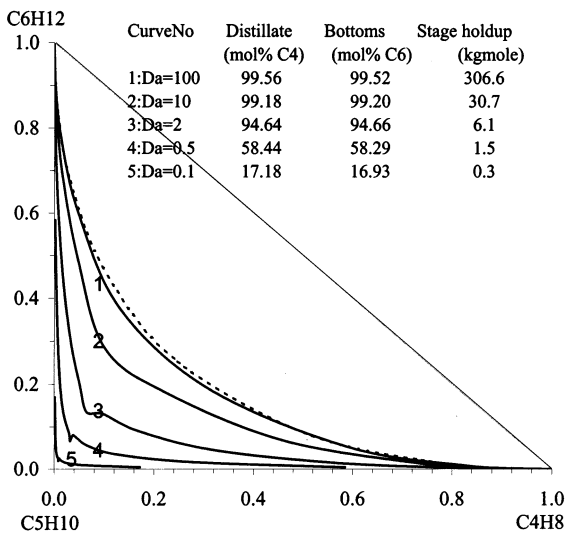

Fig. 3. Metathesis of 2-pentene. Simulation results for the specifications in Table 3 at several values of Da. The dashed line represents the phase and reaction equilibrium curve.

2. Initialize liquid compositions $x_{j,i}$ for the column by using the feed composition (averaged over all feeds) or the last converged simulation. For the *heat effects model*, it is better to use the converged simulation result from the *non-heat effects model* as an initialization.
3. Calculate vapor compositions $y_{j,i}$ and temperature T_j on stage j through the bubble point flash calculation.
4. Calculate liquid enthalpy h_j^L and vapor enthalpy h_j^V on stage j (e.g. by using DISTIL thermodynamic package; refer to Appendix B for details).
5. Calculate the liquid and vapor rates throughout the column. For *non-heat effects model* simulation, the Eqs. (A1), (A2), (A3), (A4), (A5), (A6), (A7), (A8), (A9), (A10), (A11) and (A12) in Appendix A are used to calculate V_j and L_j. For *heat effects model* simulation, Eqs. (A18), (A19), (A20), (A21), (A22), (A23), (A24) and (A25) in Appendix A are used to calculate V_j and L_j.
6. Calculate all the derivatives $dx_{j,i}/d\tau$ or $dx_{j,i}/d\zeta$ (Eq. (1) or Eq. (2)), then calculate the residual from the average of the absolute value of all the derivatives $dx_{j,i}/d\tau$ or $dx_{j,i}/d\zeta$.
7. Check if the residual is less than the specified error tolerance (e.g. 1.0×10^{-4}):If YES, converged steady-state solution is obtained, then go to 8. If NO, predict next $x_{j,i}$ by calling the integration routine, then go to 3.
8. Output the composition and temperature profiles of the column. If *non-heat effects model*, calculate condenser heat duty and reboiler heat duty.

4. Examples

To illustrate the features of these simulation strategies, three examples representing diverse applications are described below:

- metathesis of 2-pentene;
- MTBE synthesis;
- ethylene glycol.

4.1. Example 1: metathesis of 2-pentene

This is a class of reactions which are ideally suited for reactive distillation applications. The metathesis of 2-pentene to form 2-butene and 3-hexene is an equimolar and reversible reaction, as shown in Eq. (8).

$$2C_5H_{10} \Leftrightarrow C_4H_8 + C_6H_{12} \tag{8}$$

The rate model is

$$r = k_f\left(a_{C_5H_{10}}^2 - \frac{a_{C_4H_8}a_{C_6H_{12}}}{K_{eq}}\right) \tag{9}$$

The reaction equilibrium constant and rate constant are taken from Okasinski and Doherty (1998) as shown in Eqs. (10) and (11).

$$K_{eq} = 0.25 \tag{10}$$

$$k_f = 1.0661 \times 10^5 \exp(-3321.2/T)\ \text{h}^{-1}, \quad T(K) \tag{11}$$

The normal boiling point of C_5H_{10} is chosen as the reference temperature for the calculation of $k_{f,ref}$, giving a value of 2.328 h^{-1}.

At atmospheric pressure, this system has ideal vapor–liquid equilibrium and a negligible heat of reaction. We use the *non-heat effects model and constant molar holdup distribution simulation strategy* to study the transition behavior from the nonreactive to the equilibrium reactive limits. The specifications for the simulation are taken from the design results of Okasinski and Doherty (see figure 9 of Okasinski & Doherty, 1998), as shown in Table 3. The total holdup for the column, which is divided equally among all the stages,

will change with different values of Da. The simulation results at several values of Da are shown in Fig. 3.

Fig. 3 shows that the column profile moves toward the phase and reaction equilibrium curve as the Damköhler number increases. At Da = 100, the column profile is very close to the phase and reaction equilibrium curve, and high purity C_4H_8 and C_6H_{12} products are obtained from a pure C_5H_{10} feed. At Da = 0.1, the extent of reaction on each column stage was not significant and the reactive column produced low purity C_4H_8 and C_6H_{12} products.

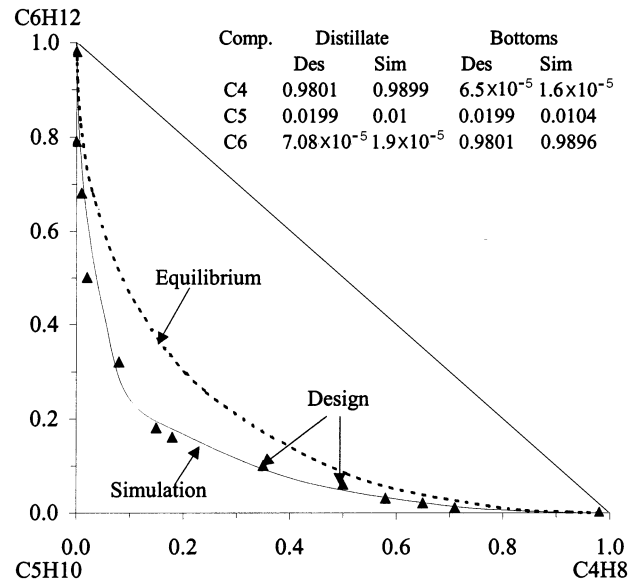

Fig. 4. Metathesis of 2-pentene. Comparison between our simulation results (solid line) and design results (filled triangles) of Okasinski and Doherty (1998). Da = 7.

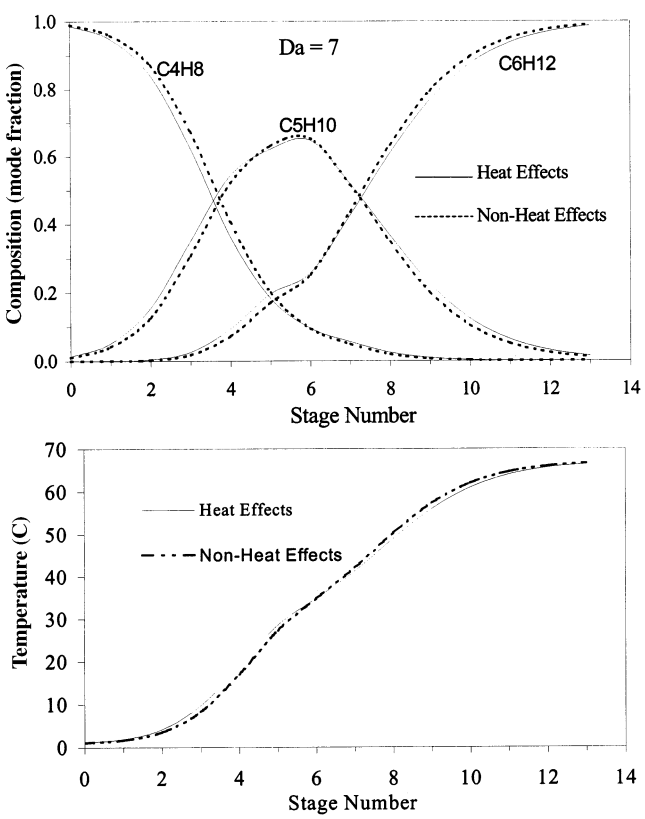

Fig. 5. Comparison of column profiles between the two simulation strategies. Da = 7. (a) Composition profile; (b) temperature profile.

A small value of Da implies one or more of the following conditions: a slow forward rate; small liquid holdups; or a large feed flow rate. In our definition of Da the reference rate constant is a fixed value, therefore, changes of the Damköhler number imply changes of the holdups on each reactive stage or a change of feed flow rate. In a practical operation, it is not realistic to have a large volume holdup on the stages. For this example, the stage volume holdup is approximately 30 cubic meters at Da = 100. Therefore, we need to reduce the Damköhler number from the large value that is characteristic of reaction equilibrium to a smaller value representing a realistic stage holdup. Now we take the Damköhler number as Da = 7 and specifications in Table 3. To match the design model assumptions made by Okasinski and Doherty (1998), the *non-heat effects model and constant molar holdup distribution simulation strategy* is used to check the design results. Fig. 4 shows the comparison between our simulation and the design results of Okasinski and Doherty (see Fig. 9 of Okasinski & Doherty, 1998), and as can be seen the two are in good agreement.

Although the heat of reaction for this reaction can be ignored, we used the *heat effects model and constant molar holdup distribution simulation strategy* to check the effects of the non-constant latent heats. Here we specify the liquid distillate rate (L_D) instead of reboil ratio in Table 3 and keep the same liquid distillate rate as that value obtained with the *non-heat effects model and constant molar holdup distribution simulation strategy*. The comparisons of column profiles between the two simulation strategies are shown in Fig. 5.

Fig. 5 shows no obvious heat effects for this system. The *heat effects model* gives the condenser heat duty ($Q_c = -5.7238 \times 10^6$ kJ h^{-1}), the reboiler heat duty ($Q_r = 5.7312 \times 10^6$ kJ h^{-1}) and the reboil ratio ($s = 3.97$) for a feed rate of 100 kmol of C_5H_{10} h^{-1}.

In addition, the *heat effects model and constant molar holdup distributions simulation strategy* is used to investigate the influence of reflux ratio on conversion of the C_5H_{10} in the column, shown in Fig. 6. The specification variables for the simulation are total number of stages, Da, feed stage, feed compositions, feed rate, and distillate rate, given in Fig. 6.

Fig. 6 shows that the conversion of C_5H_{10} increases with increasing reflux ratio at each constant value of Da. The open circle in the figure indicates the base-case design. Under the condition of a fixed value of distillate rate, the high reflux ratio means high liquid and vapor

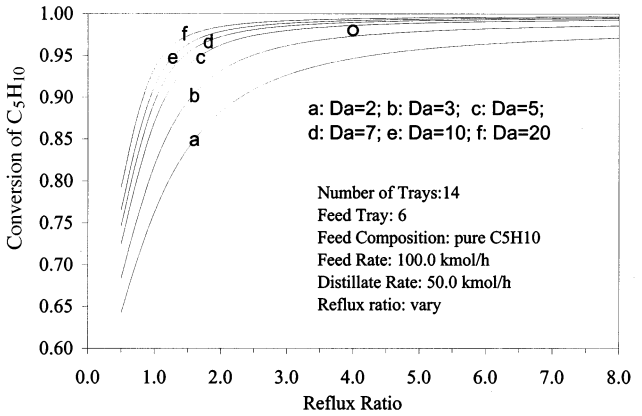

Fig. 6. Metathesis of 2-pentene. Influence of reflux ratio on the conversion of C_5H_{10} for different Da. The open circle represents the base-case design given in Table 3 and shown in Fig. 4.

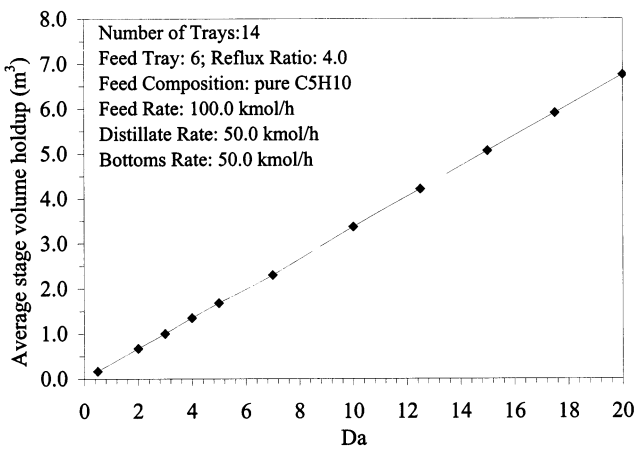

Fig. 7. Metathesis of 2-pentene. Average stage volume holdup for different Da.

loads within the column, i.e. high reboiler and condenser heat duties. So this result gives us insight into what is an economical reflux ratio for the column to satisfy the specifications of both products for a fixed value of Da.

The changes of average stage volume holdup with the Damköhler number are shown in Fig. 7. It shows that the practical range of Da is $1 < Da < 5$.

4.2. Example 2: MTBE synthesis

Methyl *t*-butyl ether (MTBE) is a chemical made using reactive distillation technology. The reactive mixture considered is isobutene reacting with methanol to produce the desired product MTBE, in the presence of an inert component, *n*-butane (DeGarmo, Parulekar & Pinjala, 1992):

$$i\text{-Butene} + \text{MeOH} \Leftrightarrow \text{MTBE} \quad (12)$$

The rate model is

$$r = k_f\left(a_{i\text{-butene}}a_{\text{MeOH}} - \frac{a_{\text{MTBE}}}{K_{\text{eq}}}\right) \quad (13)$$

The reaction equilibrium constant and rate constant are taken from Eqs. (25) and (32) in Venimadhavan et al. (1994).

$$K_{\text{eq}} = 8.33 \times 10^{-8}\exp(6820.0/T) \quad (14)$$

$$k_f = 4464\exp(-3187.0/T)\ \text{h}^{-1} \quad (15)$$

where T is in Kelvin. The boiling point (at 11 atm) of *i*-butene is chosen as the reference temperature (328.15 K) for the calculation of $k_{f,\text{ref}}$ (0.4882h^{-1}). The heat of reaction is -42.705 kJ mol^{-1} (Al-Jarallah, Lee & Siddiqui, 1988).

The liquid-phase activity coefficients are well represented by the Wilson equation. The thermodynamic data for this system are given in Appendix C.

The column configuration and feed specifications for the simulation are taken from Fig. 1 of Jacobs and Krishna (1993), as shown in Fig. 8. In this column, we specify the methanol feed location at stage 9, the mixed butenes (isobutene and *n*-butane) feed location at stage 10, constant bottoms rate of 709.2 kmol h^{-1}. The value of Da is specified and then used to calculate the total reactive molar holdup for the column, which is then divided equally among all the reactive stages (3–10). Using the *heat effects model*, the influence of reboil ratio on conversion of isobutene for different Da is shown in Fig. 9. As in the previous examples, it shows that the conversion increases with increasing Damköhler number. Now we keep the reboil ratio constant and equal to 6, $B = 709.2$ kmol h^{-1}, $Da = 100$ (reaction equilibrium column) and the same mixed butenes (isobutene and n-butane) feed location; and

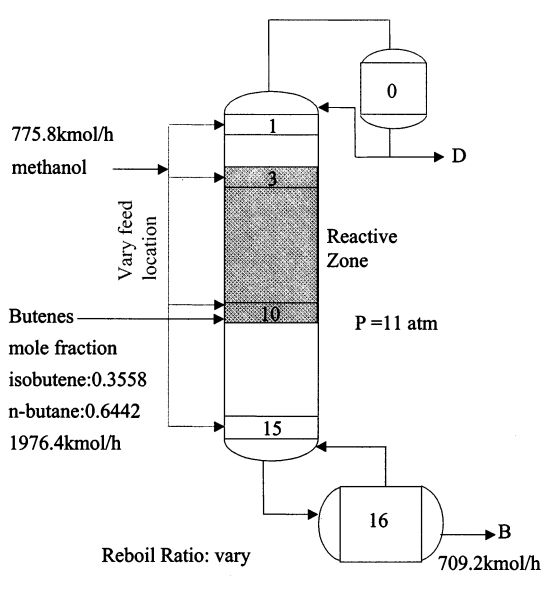

Fig. 8. Column configuration and feed specifications for MTBE system.

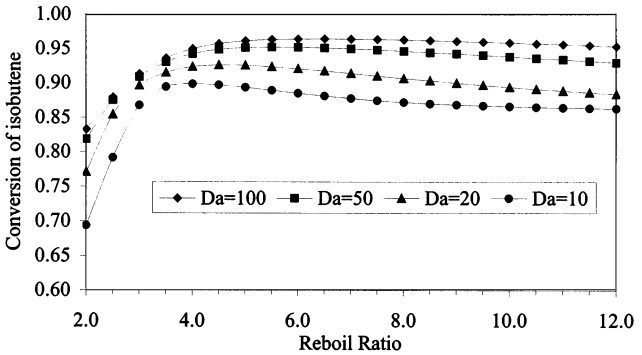

Fig. 9. Influence of reboil ratio on conversion of isobutene for different Da. Simulation with the *heat effects model*.

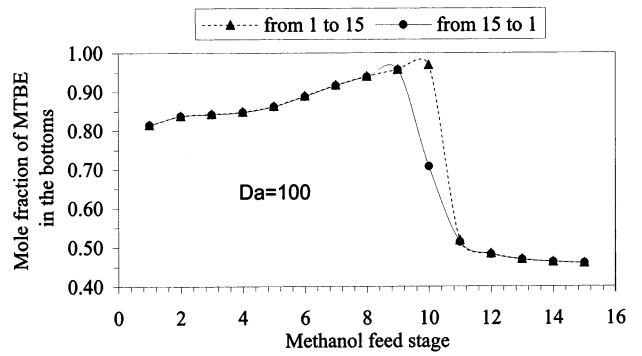

Fig. 10. Steady-state multiplicity. Da = 100. Stages 0–2 and 11–16, non-reactive; stages 3–10, reactive with constant molar holdup. Simulation with the *heat effects model*.

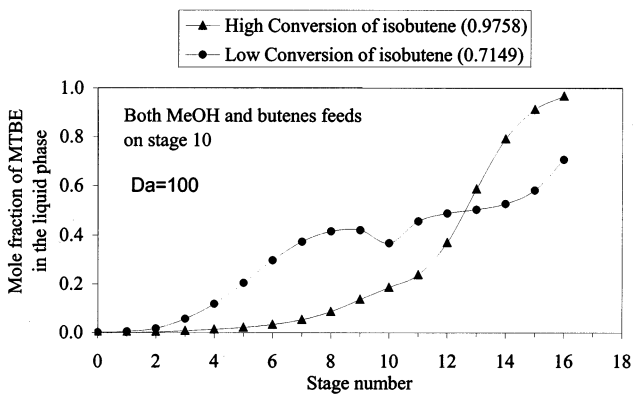

Fig. 11. Composition profiles for the multiple solutions. Da = 100.

sequentially move the methanol feed location down the column from stage 1 to stage 15 and up again. The forward/backward branches of steady-states are shown in Fig. 10. It was found that multiple steady states are obtained for the case where both methanol and mixed butenes are fed to stage 10. These results are similar to those found by Jacobs and Krishna (1993), although the details are slightly different because of differences in physical property models and simulation/modeling strategies.

The resulting composition profiles for this case are shown in Fig. 11. It shows that widely different composition profiles and conversions result from identical column specifications, depending on the initial estimates provided. The equilibrium reactive residue curve map in transformed composition coordinates (Ung & Doherty, 1995a) and the calculated transformed composition profiles for the multiple solutions are given in Fig. 12. Composition profiles for the different kinds of solutions approximately follow residue curves, which have their starting point in two different regions. High conversion corresponds to residue curves starting near the n-butane–methanol azeotrope; low conversion corresponds to residue curves starting near pure isobutene.

More explanations and predictions of steady-state multiplicity in MTBE equilibrium reactive distillation have been described by several authors (e.g. Hauan, Hertzberg & Lien, 1995; Sneesby, Tadé & Smith, 1998; Mohl, Kienle, Gilles, Rapmund, Sundmacher & Hoffmann, 1999; Güttinger & Morari, 1999a,b).

Backing away from reaction equilibrium, we repeated the simulation with Da = 10, again varying the methanol feed stage locations under the same specifications as those for Fig. 10. The forward/backward branches are shown in Fig. 13. It shows that the *multiple steady states have disappeared under conditions of a column operating in the kinetic regime.*

4.3. Example 3: ethylene glycol

The production of ethylene glycol (EG) from ethylene oxide (EO) and water (W) is a non-equimolar, irreversible, exothermic reaction and can be represented as follows:

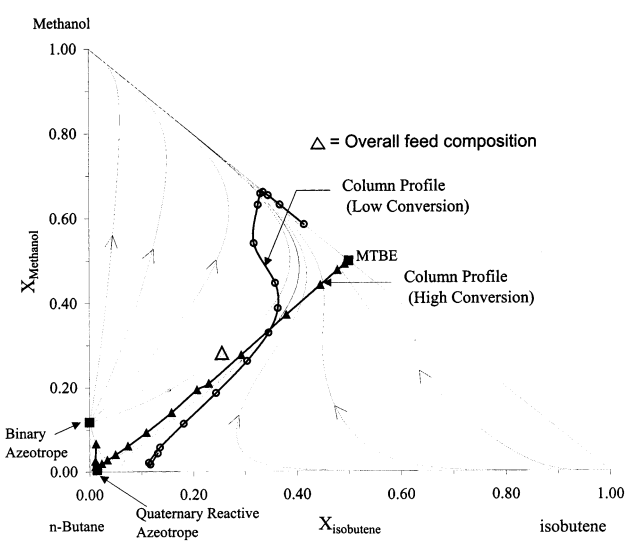

Fig. 12. Reactive residue curve map in transformed composition variables ($X_{i\text{-butene}} = (x_{\text{i-butene}} + x_{\text{MTBE}})/(1 + x_{\text{MTBE}})$, $X_{\text{methanol}} = (x_{\text{methanol}} + x_{\text{MTBE}})/(1 + x_{\text{MTBE}})$) and the calculated transformed composition profiles for the multiple solutions.

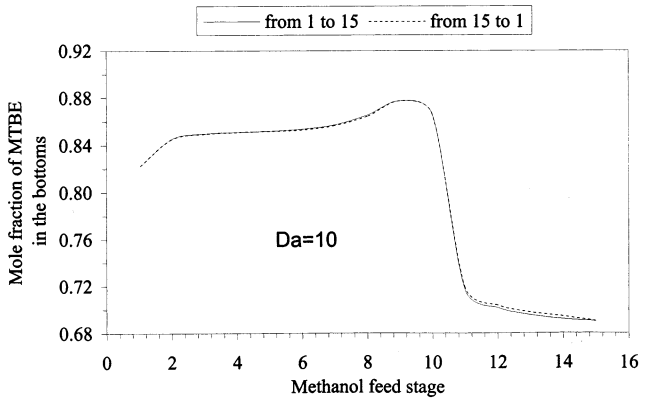

Fig. 13. Mole fraction of MTBE in the bottoms as a function of location of methanol feed stage. Da = 10. Stages 0–2 and 11–16, non-reactive; stages 3–10, reactive with constant molar holdup. Simulation with the *heat effects model*.

Table 4
Specifications for the simulation of the ethylene glycol system

Number of stages		7
Feed location		2
Feed quality		1
Feed rate		50 kmol h^{-1}
Feed composition (mole fraction)	EO	0.4878
	Water	0.5122
	EG	0.0000
Reflux ratio		1000.0
Reboil ratio		40.0
Reactive status throughout the column		Reaction occurs on the top stage only.
Liquid holdup in the reaction stage		2.14 m^3
Condenser type		c. Partial condenser

$$C_2H_4O + H_2O \Rightarrow C_2H_6O_2 \quad (16)$$

The rate model is

$$r = k_f a_{C_2H_4O} a_{H_2O} \quad (17)$$

The rate constant at pH = 10 can be obtained from Eq. (12) in Okasinski and Doherty (1998).

$$k_f = 1.9214 \times 10^{11} \exp(-9359.8/T)\ h^{-1}, \quad T(K) \quad (18)$$

The boiling point (at 15 atm) of C_2H_4O is chosen as the reference temperature (378.15 K) for the calculation of $k_{f,ref}$. Its value is 3.552 h^{-1}. The heat of reaction is -80 kJ mol^{-1} (see Table 1 of Ciric & Gu, 1994).

The thermodynamic data are given in Appendix D. The specifications for the simulation are taken from the design results of Okasinski and Doherty (see Fig. 12(b) of Okasinski & Doherty, 1998), as shown in Table 4. Since the partial condenser operation is more stable, because it provides an exit vent for light gases, we use the partial condenser model (type c in Fig. 2) for our simulation instead of the total reflux model (type b in Fig. 2) used by Okasinski and Doherty (see Figr. 12(a) of Okasinski & Doherty, 1998).

The simulation results with the *non-heat effects model* and the *heat effects model* are shown in Fig. 14. For the *non-heat effects model*, we keep the reflux ratio (1000) and the reboil ratio (40) constant. For the *heat effects model*, we keep the reflux ratio (1000) and the vapor distillate rate (0.9841 kmol h^{-1}) constant. From this figure it is difficult to see the difference between the *non-heat effects model* and the *heat effects model* (in spite of the large heat of reaction), but the liquid and vapor rates throughout the column show the difference between the models, shown in Fig. 15. The simulation summary is given in Fig. 16. This shows that the vent stream is almost pure water, and high purity EG (99.00 mol%) is produced as the bottom product.

The calculated condenser and reboiler duties are in close agreement with the results reported by Okasinski and Doherty (see Fig. 12(a) of Okasinski & Doherty, 1998). The high reflux ratio and reboil ratio cause high liquid and vapor loads within the column as shown in Fig. 15, and a high vapor-to-feed ratio (about 20). Although the ethylene glycol process features a highly exothermic reaction, the total heat rate generated by reaction within the column shown in Fig. 16 is only 5.62% that of the reboiler heat rate. Therefore, the effect of heat

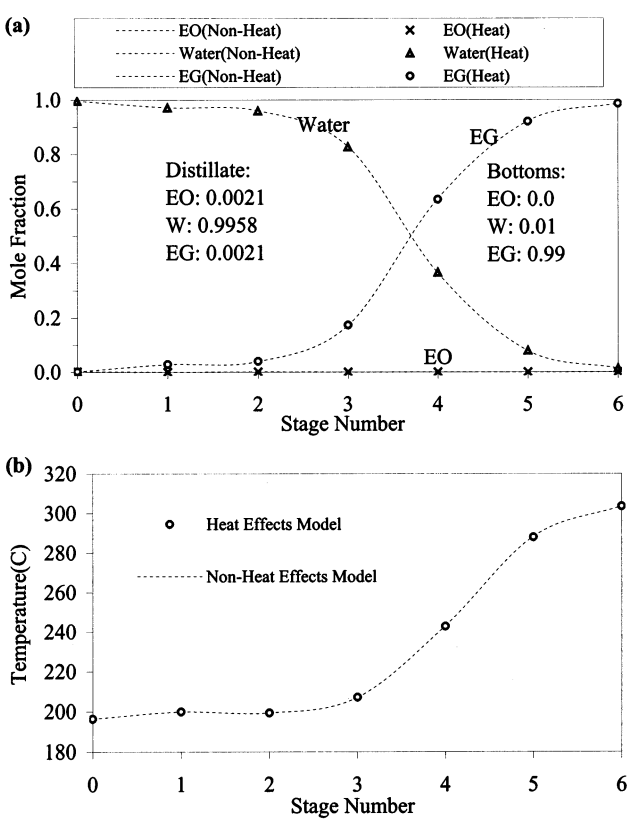

Fig. 14. Comparison of profiles using *non-heat effects model* and *heat effects model* (vapor distillate rate: 0.9841 kg mol h^{-1}; bottoms rate: 24.63 kg mol h^{-1}). Da = 7.9. (a) Composition profile; (b) temperature profile.

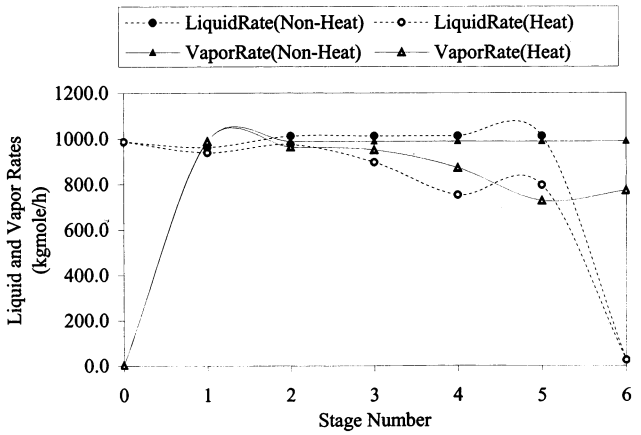

Fig. 15. Liquid and vapor rates throughout the column (vapor distillate rate: 0.9841 k mol h^{-1}; bottoms rate: 24.63 k mol h^{-1}). Da = 7.9.

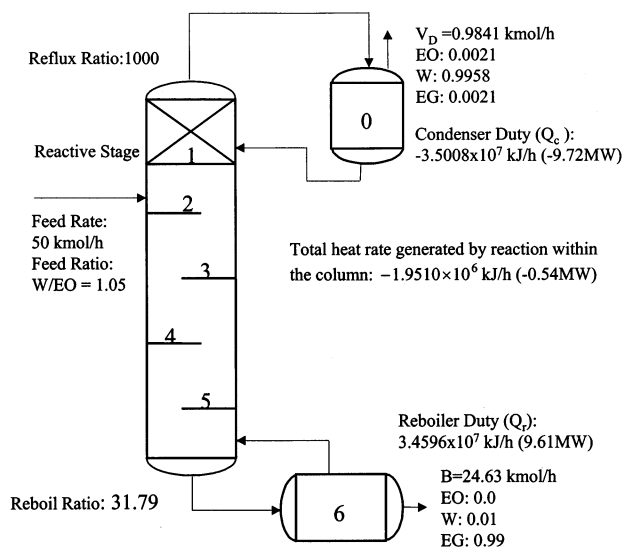

Fig. 16. Simulation summary with the *heat effects model* for ethylene glycol system. Compositions are reported as mole fractions. Da = 7.9.

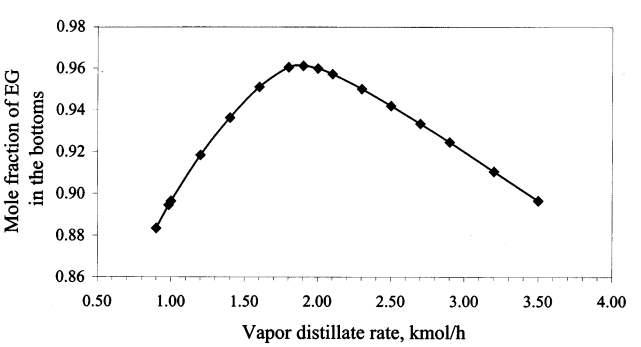

Fig. 17. Influence of vapor distillate rate on the purity of EG in the bottoms. Simulation with the *heat effects model*.

of reaction on the simulation results is relatively small, as shown in Fig. 14.

To investigate the effect of a side reaction on the selectivity and product purity, a possible side reaction of diethylene glycol (DEG) was added as follows:

$$C_2H_4O + C_2H_6O_2 \Rightarrow C_4H_{10}O_3 \quad (19)$$

The side-reaction rate expression is

$$r = k_f a_{C_2H_4O} a_{C_2H_6O_2} \quad (20)$$

We assume that the pre-exponential factor in the side-reaction rate constant (Eq. (21)) is twice that in the main reaction (Eq. (18)) and their activation energies are the same (Ciric & Gu, 1994). Therefore, the side-reaction rate constant is

$$k_f = 2.8428 \times 10^{11} \exp(-9359.8/T)\ h^{-1}, \quad T(K) \quad (21)$$

The boiling point (at 15 atm) of C_2H_4O is chosen as the reference temperature (378.15 K) for the calculation of $k_{f,ref}$ (3.552 h^{-1}) using the rate constant of the main reaction. The heat of reaction is −13.1 kJ mol^{-1} (see Table 1 of Ciric & Gu, 1994).

Using the same specifications and column configuration as described in Fig. 16, the simulation results with *the heat effects model* show that this column produces product purities of (bottoms W: 5.76 mol%; EG: 89.45 mol%; DEG: 4.79 mol%) which includes significant water and DEG. For these calculations we held the reflux ratio (1000) and the vapor distillate rate (0.9841 kmol h^{-1}) constant.

In order to improve the purities in the bottoms, we studied the influence of vapor distillate rate on the purity of EG in the bottoms for the column in Fig. 16 with the *heat effects model*, shown in Fig. 17. For these calculations we held the reflux ratio constant and equal to 1000. Fig. 17 shows the maximum purity of the EG in the bottoms (96.13 mol%) at $V_D = 1.9$ kmol h^{-1}. The simulation summary at $V_D = 1.9$ kmol h^{-1} is shown in Fig. 18. It shows that a significant amount of DEG is

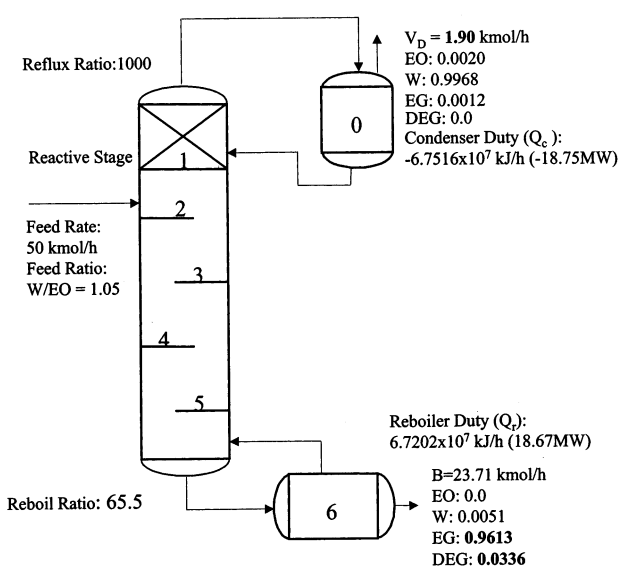

Fig. 18. Simulation summary with side reaction (DEG). Compositions are reported as mole fractions.

produced (selectivity = (moles of EG formed)/(moles of EO reacted) = 0.93) and the condenser and reboiler duties are greatly increased in this column at 15 atm.

5. Conclusions

A steady-state performance model developed from the unsteady-state form of the mass balance equations assuming phase equilibrium but not chemical equilibrium is presented. The chemical reaction terms for each stage have been formulated based on a continuous perfectly mixed stirred-tank reactor and an activity-based rate expression. The Damköhler number, which is a ratio of a characteristic liquid residence time to a characteristic reaction time, is introduced into the mathematical model. By changing the Damköhler number, the transition behavior from the nonreactive to the equilibrium reactive limits can be calculated, and provides insight into the range of values of Da for realistic column operation.

Based on the model type and the holdup distribution type on the reactive stages, the four simulation strategies were proposed: (1) non-heat effects model and constant holdup distributions simulation; (2) non-heat effects model and non-constant holdup distributions simulation; (3) heat effects model and constant holdup distributions simulation; (4) heat effects model and non-constant holdup distributions simulation. These simulation strategies, when coupled with current equilibrium and kinetic design techniques (Barbosa & Doherty, 1988a,b; Buzad & Doherty, 1994, 1995; Ciric & Gu, 1994; Huss, Song, Malone & Doherty, 1997; Huss, Chen, Malone & Doherty, 1999; Okasinski & Doherty, 1998; Bessling et al., 1997; Hauan et al., 2000; Lee et al., 2000a,b; Melles, Grievink & Schrans, 2000) are an efficient tool for developing conceptual designs and analyses for kinetically controlled columns. The main features of this simulation strategy are as follows: (a) transition from 'slow' to 'fast' reaction depends on parameters such as the feed rate, the holdup and the rate constant. These effects are captured simply in a one dimensionless group — the Damköhler number. (b) The analysis takes into account side-reaction, effects of heat of reaction, non-constant latent heat effects, a distribution of liquid holdups on the reactive stages and the presence of hybrid sections in a column. (c) Comprehensive computational studies with Damköhler number can be used to determine what column conditions are required to approach the equilibrium limit corresponding to large holdups or fast reactions. (d) Sensitivity calculations such as conversion vs. reflux ratio, Damköhler number, reboil ratio, distillate rate, etc. can provide an optimal range of operability.

The metathesis of 2-pentene, production of MTBE and ethylene glycol reactive distillation are used to illustrate that the numerical methods are efficient and robust, and these simulation strategies can be used for solving a variety of reactive distillation problems.

6. Notation

$a_{j,i}$	activity of component i on stage j
B	bottoms flow rate (kmol h^{-1})
C	number of components
D	distillate flow rate (kmol h^{-1})
Da	Damköhler number for whole column
F	total feed flow rate to entire column (kmol h^{-1})
F_j	feed flow rate of stage j (zero for non-feed stages) (kmol h^{-1})
H_j	holdup of stage j (kmol)
H_T	total holdup for the entire column (kmol)
H_T^R	total holdup with reaction(s) for the entire column (kmol)
ΔH^R	heat of reaction (kJ $kmol^{-1}$)
$\hat{h}^V$	partial molar enthalpy of vapor (kJ $kmol^{-1}$)
$\hat{h}^L$	partial molar enthalpy of liquid (kJ $kmol^{-1}$)
K_{eq}	thermodynamic reaction equilibrium constant for a single reaction
K_r	thermodynamic reaction equilibrium constant of reaction r
$k_{f,r}$	forward rate constant of reaction r (h^{-1})
$k_{f,ref}$	forward rate constant evaluated at boiling point of a reference component in the system (h^{-1})
L_D	liquid distillate (kmol h^{-1})
L_j	liquid rate of stage j (kmol h^{-1})
N	total number of stages
P^{sat}	saturated vapor pressure (Pa)
R	total number of reactions
R_j	total rate of generation of moles on stage j (kmol h^{-1})
r	reflux ratio
s	reboil ratio
t	time (h)
V_D	vapor distillate (kmol h^{-1})
V_j	vapor rate of stage j (kmol h^{-1})
$x_{j,i}$	liquid mole fraction of component i on stage j
$y_{j,i}$	vapor mole fraction of component i on stage j
$z_{j,i}$	feed mole fraction of component i on stage j

Greek letters

$\varepsilon_{j,r}$	the extent of reaction r on stage j (mole reacted)/(mole of mixture × time)
$\delta_j = 0$	stage j has no reactions
$\delta_j = 1$	stage j has reactions
q_j	feed quality of stage j
τ	dimensionless warped time
$v_{r,I}$	stoichiometric coefficient of component i in reaction r
$v_{r,T}$	sum of the stoichiometric coefficients of reaction r

Subscripts

i	component number
j	stage number
r	reaction number
T	total

Superscript

f	feed
L	liquid
V	vapor
R	reaction(s)
D	distillate

Acknowledgements

The authors are grateful for financial and technical support from the sponsors of the Fortune project at the University of Massachusetts: Dow Corning Corp., DuPont Company, Eastman Chemical Company, ICI, Shell International Chemical BV, Union Carbide Corp., Hyprotech Ltd.

Appendix A. Liquid and vapor rates within the column

For *non-heat effects model*, the assumptions (3) and (4) can guarantee that the change in the liquid flow rate in each section of the column is only due to changes in the total number of moles by reaction, and the vapor flow rate is constant in each section of the column. In this case, the reflux ratio, reboil ratio, D and B are not independent variables. Combining the total mass balance and assumptions (1)–(7) yields B and D:

$$B = \frac{rF_0 + \sum_{j=1}^{N-1}(r+q_j)F_j + (1+r)F_N + (1+r)\sum_{j=0}^{N} R_j - R_0}{r+s+1} \tag{A1}$$

$$D = \frac{(1+s)F_0 + \sum_{j=1}^{N-1}(1+s-q_j)F_j + sF_N + s\sum_{j=0}^{N} R_j + R_0}{r+s+1} \tag{A2}$$

where $r = L_0/D$, $s = V_N/B$, $D = V_D + L_D$. The liquid and vapor rates throughout the column can be determined by a set of algebraic equations:

Liquid phase

$$L_0 = rD \tag{A3}$$

$$L_1 = rD + q_1F_1 + R_1 \tag{A4}$$

$$L_2 = L_1 + q_2F_2 + R_2 = rD + q_1F_1 + q_2F_2 + R_1 + R_2 \tag{A5}$$

.

.

.

$$L_{N-1} = L_{N-2} + q_{N-1}F_{N-1} + R_{N-1} = (rD + q_1F_1 + q_2F_2 + \cdots + q_{N-1}F_{N-1}) + (R_1 + R_2 + \cdots + R_{N-1}) \tag{A6}$$

$$L_N = B \tag{A7}$$

Vapor phase

$$V_0 = V_D \tag{A8}$$

$$V_1 = (r+1)D - R_0 - F_0 \tag{A9}$$

$$V_2 = V_1 + (q_1 - 1)F_1 = (r+1)D + (q_1 - 1)F_1 - R_0 - F_0 \tag{A10}$$

.

.

.

$$V_{N-1} = V_{N-2} + (q_{N-2} - 1)F_{N-2} = (r+1)D + (q_1 - 1)F_1 + \cdots + (q_{N-2} - 1)F_{N-2} - R_0 - F_0 \tag{A11}$$

$$V_N = sB \tag{A12}$$

For *heat effects model*, the energy balance and mass balance equations are used to calculate the liquid and vapor rates throughout the column. When we do energy balance, we will not introduce a term from the rate of generation of heat by reaction since this will arise naturally as an enthalpy change due to changing composition. The elemental reference state is used to compute the mixture enthalpies (refer to Appendix B for details of enthalpy datum and calculations). In the steady state, the enthalpy balance enclosing stage j ($j \neq 0, N$) is given by

$$V_{j+1}\sum_{i=1}^{C}(y_{j+1,i}\hat{h}^V_{j+1,i}) + L_{j-1}\sum_{i=1}^{C}(x_{j-1,i}\hat{h}^L_{j-1,i}) + F_j\sum_{i=1}^{C}(z_{j,i}\hat{h}^f_{j,i}) - V_j\sum_{i=1}^{C}(y_{j,i}\hat{h}^V_{j,i}) - L_j\sum_{i=1}^{C}(x_{j,i}\hat{h}^L_{j,i}) = 0 \tag{A13}$$

Use of the component-material balance to eliminate one of the component-flow rates ($L_jx_{j,i}$) yields

$$V_{j+1}=\Bigg(V_j\sum_{i=1}^{C}y_{j,i}(\hat{h}^V_{j,i}-\hat{h}^L_{j,i})-F_j\sum_{i=1}^{C}z_{j,i}(\hat{h}^f_{j,i}-\hat{h}^L_{j,i})-L_{j-1}\sum_{i=1}^{C}x_{j-1,i}(\hat{h}^L_{j-1,i}-\hat{h}^L_{j,i})+\sum_{i=1}^{C}R_{j,i}\hat{h}^L_{j,i}\Bigg)\Bigg/\sum_{i=1}^{C}y_{j+1,i}(\hat{h}^V_{j+1,i}-\hat{h}^L_{j,i}) \tag{A14}$$

where

$$R_{j,i}=\delta_j H_j\sum_{r=1}^{R}(v_{r,i}\varepsilon_{j,r}),\quad j=0,1,\ldots,N;$$

$$i=1,2,\ldots,C;\quad r=1,2,\ldots,R \tag{A15}$$

By using Eq. (A15) and definition of the heat of reaction ($\Delta H^R_{j,r}=\Sigma^C_{i=1}(v_{r,i}\hat{h}^L_{j,i})$), the item $\Sigma^C_{i=1}R_{j,i}\hat{h}^L_{j,i}$ in Eq. (A14) is restated in the following equivalent form:

$$\begin{aligned}\sum_{i=1}^{C}R_{j,i}\hat{h}^L_{j,i}&=\sum_{i=1}^{C}\delta_j H_j\sum_{r=1}^{R}(v_{r,i}\varepsilon_{j,r})\hat{h}^L_{j,i}\\&=\delta_j\sum_{r=1}^{R}\Bigg[\sum_{i=1}^{C}(v_{r,i}\hat{h}^L_{j,i})\varepsilon_{j,r}\Bigg]H_j\\&=\delta_j H_j\sum_{r=1}^{R}(\Delta H^R_{j,r})\varepsilon_{j,r}\end{aligned} \tag{A16}$$

Substituting Eq. (A16) into Eq. (A14) gives

$$V_{j+1}=\Bigg(V_j\sum_{i=1}^{C}y_{j,i}(\hat{h}^V_{j,i}-\hat{h}^L_{j,i})-F_j\sum_{i=1}^{C}z_{j,i}(\hat{h}^f_{j,i}-\hat{h}^L_{j,i})-L_{j-1}\sum_{i=1}^{C}x_{j-1,i}(\hat{h}^L_{j-1,i}-\hat{h}^L_{j,i})+\delta_j H_j\sum_{r=1}^{R}(\Delta H^R_{j,r})\varepsilon_{j,r}\Bigg)\Bigg/\sum_{i=1}^{C}y_{j+1,i}(\hat{h}^V_{j+1,i}-\hat{h}^L_{j,i}) \tag{A17}$$

$\Delta H^R_{j,r}$ is the heat of r reaction on stage j. $\Delta H^R_{j,r}<0$ for exothermic reactions, and $\Delta H^R_{j,r}>0$ for endothermic reactions.

Based on the Eq. (A17), a set of algebraic equations is used to determine the liquid and vapor rates throughout the column as follows:

$$V_0=0 \tag{A18}$$

$$L_0=rD \tag{A19}$$

$$V_1=(r+1)D-R_0-F_0 \tag{A20}$$

$$V_2=\Bigg(V_1\sum_{i=1}^{C}y_{1,i}(\hat{h}^V_{1,i}-\hat{h}^L_{1,i})-F_1\sum_{i=1}^{C}z_{1,i}(\hat{h}^f_{1,i}-\hat{h}^L_{1,i})-L_0\sum_{i=1}^{C}x_{0,i}(\hat{h}^L_{0,i}-\hat{h}^L_{1,i})+\delta_1 H_1\sum_{r=1}^{R}(\Delta H^R_{1,r})\varepsilon_{1,r}\Bigg)\Bigg/\sum_{i=1}^{C}y_{2,i}(\hat{h}^V_{2,i}-\hat{h}^L_{1,i}) \tag{A21}$$

$$L_1=L_0+V_2+F_1+R_1-V_1 \tag{A22}$$

.
.
.

$$V_{j+1}=\Bigg(V_j\sum_{i=1}^{C}y_{j,i}(\hat{h}^V_{j,i}-\hat{h}^L_{j,i})-F_j\sum_{i=1}^{C}z_{j,i}(\hat{h}^f_{j,i}-\hat{h}^L_{j,i})-L_{j-1}\sum_{i=1}^{C}x_{j-1,i}(\hat{h}^L_{j-1,i}-\hat{h}^L_{j,i})+\delta_j H_j\sum_{r=1}^{R}(\Delta H^R_{j,r})\varepsilon_{j,r}\Bigg)\Bigg/\sum_{i=1}^{C}y_{j+1,i}(\hat{h}^V_{j+1,i}-\hat{h}^L_{j,i}) \tag{A23}$$

$$L_j=L_{j-1}+V_{j+1}+F_j+R_j-V_j \tag{A24}$$

.
.
.

$$L_N=B \tag{A25}$$

The following expressions are used to calculate the condenser and reboiler heat duties (Q_c and Q_r):

$$Q_c=V_D h^V_{0,mix}+(L_D+L_0)h^L_{0,mix}-V_1 h^V_{1,mix}-F_0 h^f_{0,mix}-\delta_0 H_0\sum_{r=1}^{R}[(\Delta H^R_{0,r})\varepsilon_{0,r}] \tag{A26}$$

$$Q_r=V_N h^V_{N,mix}+L_N h^L_{N,mix}-L_{N-1}h^L_{N-1,mix}-F_N h^f_{N,mix}-\delta_N H_N\sum_{r=1}^{R}[(\Delta H^R_{N,r})\varepsilon_{N,r}] \tag{A27}$$

Appendix B. Enthalpy datum and calculations

The liquid phase and vapor phase enthalpies are calculated with HYCON thermodynamic package (Hyprotech Ltd., 1996). The calculation of the enthalpy of a component is based on the elemental reference state, shown in the following figure.

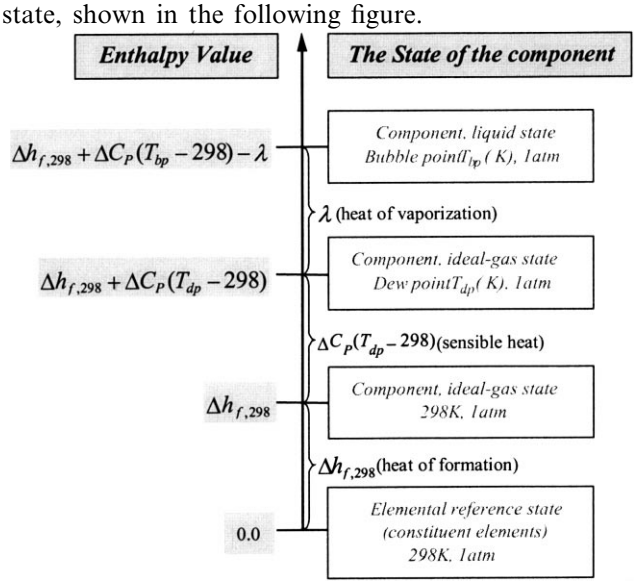

For the calculation of the enthalpy of vapor mixture and liquid mixture, the formulations are as follows:

$$h^L_{j,\text{mix}} = \sum_{i=1}^{C} x_{j,i} h^L_{j,i} + \Delta h^L_{j,\text{mix}} \quad \text{(B1)}$$

$$h^V_{j,\text{mix}} = \sum_{i=1}^{C} y_{j,i} h^V_{j,i} + \Delta h^V_{j,\text{mix}} \quad \text{(B2)}$$

where $h^L_{j,i}$ and $h^V_{j,i}$ are the enthalpies of component i in the liquid phase and the vapor phase, respectively. $\Delta h^L_{j,\text{mix}}$ and $\Delta h^V_{j,\text{mix}}$ are the mixing enthalpies in the liquid phase and the vapor phase, respectively. In HYCON thermodynamic package, $\Delta h^L_{j,\text{mix}}$ and $\Delta h^V_{j,\text{mix}}$ are ignored.

Appendix C. Thermodynamic data for MTBE system (see Table 3 of Ung & Doherty, 1995b)

Antoine vapor pressure expression:

$$\ln P^{\text{sat}} = A + \frac{B}{T + C}, \quad P^{\text{sat}} \text{ in Pa, } T \text{ in K.}$$

	Isobutene	Methanol	MTBE	*n*-Butane
A	20.6455	23.4999	20.7162	20.57097
B	−2125.7489	−3643.3136	−2571.5846	−2154.8973
C	−33.160	−33.434	−48.406	−34.42

Wilson binary interaction parameters:

	Isobutene	Methanol	MTBE	*n*-Butane
Isobutene	0	2576.8532	271.5669	0
Methanol	169.9953	0	−406.3902	382.3429
MTBE	−60.1085	1483.2478	0	0
n-Butane	0	2283.8726	0	0

Appendix D

Thermodynamic data for ethylene glycol system (see Appendix D of Okasinski & Doherty, 1998)

Antoine vapor pressure expression:

$$\ln P^{\text{sat}} = A + \frac{B}{T + C}, \quad P^{\text{sat}} \text{ in Pa, } T \text{ in K.}$$

	EO	Water	EG	DEG
A	21.3066	23.2256	25.1431	23.8578
B	−2428.2	−3835.18	−6022.18	−6085.25
C	−35.388	−45.34	−28.25	−26.15

Wilson binary interaction parameters:

	EO	Water	EG	DEG
EO	0	1905.77	635.82	635.82
Water	124.96	0	−1265.74	−1265.74
EG	−79.47	1266.01	0	0
DEG	−79.47	1266.01	0	0

References

Abufares, A. A., & Douglas, P. L. (1995). Mathematical modelling and simulation of an MTBE catalytic distillation process using SPEEDUP and ASPENPLUS. *Transactions of the Institute of Chemical Engineers A*, *73*, 3.

Alejski, K., Szymanowski, J., & Bogacki, M. (1988). The application of a minimization method for solving reacting-distillation problems. *Computers & Chemical Engineering*, *12*(8), 833.

Al-Jarallah, A. M., Lee, A. K. K., & Siddiqui, M. A. B. (1988). Kinetics of methyl tertiary butyl ether synthesis catalyzed by sulphuric acid. *Chemical Engineering Journal*, *39*, 169.

Barbosa, D., & Doherty, M. F. (1988a). Design and minimum reflux calculations for single-feed multicomponent reactive distillation columns. *Chemical Engineering Science*, *43*, 1523.

Barbosa, D., & Doherty, M. F. (1988b). Design and minimum reflux calculations for double-feed multicomponent reactive distillation columns. *Chemical Engineering Science*, *43*, 2377.

Bessling, B., Schembecker, G., & Simmrock, K. H. (1997). Design of processes with reactive distillation line diagrams. *Industrial & Engineering Chemistry Research*, *36*, 3032.

Bessling, B. (1999). Experimental and computational screening methods for reactive distillation. *FOCAPD 99*, Breckenridge, Colorado.

Bogacki, M. B., Alejski, K., & Szymanowski, J. (1989). The fast method of the solution of a reacting distillation problem. *Computers & Chemical Engineering*, *13*(9), 1081.

Buzad, G., & Doherty, M. F. (1994). Design of three component kinetically controlled reactive distillation columns using fixed point methods. *Chemical Engineering Science*, *49*, 1947.

Buzad, G., & Doherty, M. F. (1995). New tools for the design of kinetically controlled reactive distillation columns for ternary mixtures. *Computers & Chemical Engineering*, *19*, 395.

Carra, S., Morbidelli, M., Santacesaria, E., & Buzzi, G. (1979). Synthesis of propylene oxide from propylene chlorohydrins. 2. Modeling of the distillation with chemical reaction unit. *Chemical Engineering Science*, *34*, 1133.

Chang, Y. A., & Seader, J. D. (1988). Simulation of continuous reactive distillation by a homotopy-continuation method. *Computers & Chemical Engineering*, *12*(12), 1243.

Ciric, A. R., & Gu, D. (1994). Synthesis of nonequilibrium reactive distillation processes by MINLP optimization. *American Institute of Chemical Engineers Journal*, *40*, 1479.

Ciric, A. R., & Miao, P. (1994). Steady state multiplicity in an ethylene glycol reactive distillation column. *Industrial & Engineering Chemistry Research*, *33*(11), 2738.

DeGarmo, J. L., Parulekar, V. N., & Pinjala, V. (1992). Consider reactive distillation. *Chemical Engineering Progress*, *88*(3), 43.

Doherty, M. F., & Buzad, G. (1992). Reactive distillation by design. *Transactions of the Institute of Chemical Engineers*, *70A*, 448.

Espinosa, J., Aguirre, P., & Perez, G. (1995a). Product composition regions of single-feed reactive distillation columns: mixtures containing inerts. *Industrial & Engineering Chemistry Research*, *34*, 853.

Espinosa, J., Aguirre, P., & Perez, G. (1995b). Some aspects in the design of multicomponent reactive distillation columns including nonreacting species. *Chemical Engineering Science*, *50*, 469.

Espinosa, J., Aguirre, P., Frey, T., & Stichlmair, J. (1999). Analysis of finishing reactive distillation columns. *Industrial & Engineering Chemistry Research*, *38*, 187.

Gani, R., Perregaard, J., & Johansen, H. (1990). Simulation strategies for design and analysis of complex chemical processes. *Transactions of the Institute of Chemical Engineers A*, *68*, 407.

Gani, R., Sørensen, E. L., & Perregaard, J. (1992). Design and analysis of chemical processes through DYNSIM. *Industrial & Engineering Chemistry Research*, *31*(1), 244.

Gear, C. W. (1971). *Numerical Initial Value Problems in Ordinary Differential Equations*. Englewood Cliffs, NJ: Prentice Hall.

Giessler, S., Danilov, R. Y., Pisarenko, R. Y., Serafimov, L. A., Hasebe, S., & Hashimoto, I. (1998). Feasibility study of reactive distillation using the analysis of the statics. *Industrial & Engineering Chemistry Research*, *37*, 4375.

Grosser, J. H., Doherty, M. F., & Malone, M. F. (1987). Modeling of reactive distillation systems. *Industrial & Engineering Chemistry Research*, *26*, 983.

Güttinger, T. E., & Morari, M. (1999a). Predicting multiple steady state in equilibrium reactive distillation. 1. Analysis of nonhybrid systems. *Industrial & Engineering Chemistry Research*, *38*, 1633.

Güttinger, T. E., & Morari, M. (1999b). Predicting multiple steady state in equilibrium reactive distillation. 2. Analysis of hybrid systems. *Industrial & Engineering Chemistry Research*, *38*, 1649.

Hauan, S., & Lien, K. M. (1998). A phenomena based design approach to reactive distillation. *Transactions of the Institute of Chemical Engineers A*, *76*, 396.

Hauan, S., Hertzberg, T., & Lien, K. M. (1995). Why methyl *tert*-butyl ether production by reactive distillation may yield multiple solutions. *Industrial & Engineering Chemistry Research*, *34*, 987.

Hauan, S., Westerberg, A. W., & Lien, K. M. (2000). Phenomena-based analysis of fixed points in reactive separation systems. *Chemical Engineering Science*, *55*, 1053.

Higler, A., Taylor, R., & Krishna, R. (1999). The influence of mass transfer and liquid mixing on the performance of reactive distillation tray column. *Chemical Engineering Science*, *54*, 2879.

Huss, R. S., Chen, F., Malone, M. F., & Doherty, M. F. (1999). *Computer-aided tools for the design of reactive distillation systems*. Presented at ESCAPE9.

Huss, R. S., Song, W., Malone, M. F., & Doherty, M. F. (1997). Computations and experiments for the feasibility of reactive distillation. Paper 199a, *American Institute of Chemical Engineers Annual Meeting*, Los Angeles, CA.

Hyprotech Ltd. (1996). Conceptual Design Application: Version 1.1. *HYSYS Reference*. Calgary, Alta T2E 2R2, Canada.

Izarraraz, A., Bentzen, G. W., Anthony, R. G., & Holland, C. D. (1980). Solve more distillation problems. Part 9. When chemical reactions occur. *Hydrocarbon Processing*, *57*(4), 195.

Jacobs, R., & Krishna, R. (1993). Multiple solutions in reactive distillation for methyl tert-butyl ether synthesis. *Industrial & Engineering Chemistry Research*, *32*, 1706.

Jelineck, P., & Hlavacek, V. (1976). Steady state countercurrent equilibrium stage separation with chemical reaction by relaxation method. *Chemical Engineering Communication*, *2*, 79.

Komatsu, H., & Holland, C. D. (1977). A new method of convergence for solving reacting distillation problems. *Journal of Chemical Engineering of Japan*, *10*(4), 292.

Komatsu, H. (1977). Application of the relaxation method for solving reaction distillation problems. *Journal of Chemical Engineering of Japan*, *10*(3), 200.

Mahajani, S. M. (1999). Design of reactive distillation columns for multicomponent kinetically controlled reactive systemsm. *Chemical Engineering Science*, *54*, 1425.

Melles, S., Grievink, J., & Schrans, S. M. (2000). Optimisation of the conceptual design of reactive distillation columns. *Chemical Engineering Science*, *55*, 2089.

Mohl, K., Kienle, A., Gilles, E., Rapmund, P., Sundmacher, K., & Hoffmann, U. (1999). Steady-state multiplicities in reactive distillation columns for the production of fuel ethers MTBE and TAME: theoretical analysis and experimental verification. *Chemical Engineering Science*, *54*, 1029.

Lee, J. W., Hauan, S., Lien, K. M., & Westerberg, A. W. (2000a). A graphical method for designing reactive distillation columns. 1. The Ponchon–Savarit method. *Proceedings of the Royal Society of London*, in press.

Lee, J. W., Hauan, S., Lien, K. M., & Westerberg, A. W. (2000b). A graphical method for designing reactive distillation columns. 2. The McCabe–Thiele method. *Proceedings of the Royal Society of London*, in press.

Nisoli, A., Malone, M. F., & Doherty, M. F. (1997). Attainable regions for reaction with separation. *American Institute of Chemical Engineers Journal*, *43*, 374.

Nelson, P. A. (1971). Countercurrent equilibrium stage separation with reaction. *American Institute of Chemical Engineers Journal*, *17*(5), 1043.

Okasinski, M. J., & Doherty, M. F. (1998). Design method for kinetically controlled, staged reactive distillation colums. *Industrial & Engineering Chemistry Research*, *37*, 2821.

Papalexandri, K. P., & Pistikopoulos, E. N. (1996). Generalized modular representation framework for process synthesis. *American Institute of Chemical Engineers Journal*, *42*, 1010.

Perregaard, J., Pedersen, B. S., & Gani, R. (1992). Steady state and dynamic simulation of complex chemical processes. *Transactions of the Institute of Chemical Engineers A*, *70*, 99.

Pilavachi, P. A., Schenk, M., Perrez-Cisneros, E., & Gani, R. (1997). Modeling and simulation of reactive distillation operations. *Industrial & Engineering Chemistry Research*, *36*(8), 3188.

Sørensen, E. L., Johansen, H., Gani, R., & Fredenslund, A.a. (1990). *Process Technology Proceedings*, vol. 9 (p. 13). Amsterdam: Elsevier.

Ruiz, C. A., Basualdo, M. S., & Scenna, N. J. (1995). Reactive distillation dynamic simulation. *Transactions of the Institute of Chemical Engineers A*, *73*, 363.

Rev, E. (1994). Reactive distillation and kinetic azeotropy. *Industrial & Engineering Chemistry Research*, *33*, 2174.

Sivasubramanian, M. S. & Boston, J. F. (1990). The heat and mass transfer rate-based approach for modeling multicomponent separation processes. *Computer Applications in Chemical Engineering*, 331.

Sneesby, M. G., Tadé, M. O., & Smith, T. N. (1998). Mechanistic interpretation of multiplicity in hybrid reactive distillation: physically realizable cases. *Industrial & Engineering Chemistry Research*, *37*, 4424.

Sundmacher, K., Rihko, L. K., & Hoffmann, U. (1994). Classification of reactive distillation processes by dimensionless numbers. *Chemical Engineering Communications*, *127*, 151.

Suzuki, I., Yagi, H., Komatsu, H., & Hirata, M. (1971). Calculation of multicomponent distillation accompanied by a chemical reaction. *Journal of Chemical Engineering of Japan*, *4*(1), 26.

Tierney, J. W., & Riquelme, G. D. (1982). Calculation methods for distillation systems with reactions. *Chemical Engineering Communications*, *16*, 91.

Ung, S, & Doherty, M. F. (1995a). Synthesis of reactive distillation systems with multiple equilibrium chemical reactions. *Industrial & Engineering Chemistry Research*, *34*, 2555.

Ung, S., & Doherty, M. F. (1995b). Vapor–liquid phase equilibrium in systems with multiple chemical reactions. *Chemical Engineering Science*, *50*(1), 23.

Venimadhavan, G., Buzad, G., Doherty, M. F., & Malone, M. F. (1994). Effect of kinetics on residue curve maps for reactive distillation. *American Institute of Chemical Engineers Journal*, *40*(11), 1814.

Venkataraman, S., Chan, W. K., & Boston, J. F. (1990). Reactive distillation using ASPEN PLUS. *Chemical Engineering Progress*, *86*(8), 45.

Xu, X., & Chen, H. (1987). Simulation of distillation processes with reactions in series. *Journal of Chemistry Industry & Engineering* (*China*), *2*, 165.

Zhang, R. (1989). Simulation of distillation with simultaneous chemical reaction-modified Newton–Raphson method. *Journal of the East China Institute of Chemistry & Technology*, *15*(1), 25.